



Surface Photovoltage Monitoring of Heavy Metal Contamination on Silicon During Chemical Cleaning in IC Manufacturing

メタデータ	言語: eng 出版者: 室蘭工業大学 公開日: 2014-03-04 キーワード (Ja): キーワード (En): 作成者: 野村, 滋, 遠藤, 敏明, HUKUDA, Hisashi, JASTRZEBSKI, Lubek, LAGOWSKI, Jacek メールアドレス: 所属:
URL	http://hdl.handle.net/10258/600

Surface Photovoltage Monitoring of Heavy Metal Contamination on Silicon During Chemical Cleaning in IC Manufacturing

Shigeru NOMURA*, Toshiaki ENDOU*, Hisashi HUKUDA*,
Lubek JASTRZEBSKI** and Jacek LAGOWSKI**

Abstract

The principles and application examples of recently refined, computerized surface photovoltage (SPV) method are described. The SPV method was used to optimize cleaning efficiency and to monitor 'in-line' heavy metal contamination and charge during critical processing steps for Statistical Process Control (SPC). Examples of the optimization of various cleaning steps, effects of the purity of virgin and reused chemicals, and the surface topology on cleaning efficiency will be given together with examples of SPC monitoring of real problems in processing lines. Cleanliness of incoming chemicals is not always a limiting factor and often is not related to the cleanliness of chemicals at the point of use (in the cleaning station). This new method is capable of waferscale, non-contact mapping of metal contaminants in the bulk and on the surface with sensitivities as high as 10^{10} atoms cm^{-3} .

1. Introduction

The continuing increase of IC circuit complexity, and the reduction of critical dimension that requires reduction of gate oxide thickness, generates a need for better control of heavy metal contamination. Detection of heavy metal contaminants in silicon wafers has recently gained a great deal of attention as a critical task for cost-effective manufacturing of several-Mb integrated circuits^{1,2)}. Employing surface photovoltage (SPV) characterization methods, quantitative relationships have been established between the minority carrier diffusion length, the concentration of heavy metals added during processing and the IC yield degradation^{1,2)}. The minority carrier diffusion length, as measured directly by SPV, has become a standard parameter guiding the process engineer.

The diffusion length value L helps one to make a quick, quantitative judgement of the

* Muroran Institute of Technology.

**University of South Florida.

cleanliness of materials, tools and processes. Also, if the diffusion length drops below a critical value characteristic for a given IC process, the engineer receives a warning signal of the forthcoming yield degradation.

There is an urgent need for a fast, inexpensive, high throughput measurement method that can be used as a QC method to qualify, in realtime, cleaning processes, incoming chemicals, chemicals at point-of-use, and performance of cleaning station. We explore the application of SPV to monitor chemical cleaning. Compared to other technologies such as TXRF or AAS, the application of SPV to monitor cleaning processes is rather new, although some impressive strides have already been made.

The diffusion length of the minority carriers and the surface recombination are determined independently from the spectral dependence of the SPV signal. Surface charge is obtained from the dependence of the SPV signal on light intensity. Quantitative identification of Fe and Cr (even in the presence of other recombination centers, e. g., oxygen precipitates) was measured via changes of the lifetime during dissociation of the Fe-B and Cr-B pairs. Due to the difference in the pairing energies, characteristic of each heavy metal, pair dissociation can be selectively performed in-situ for each of the metals by a combination of light and temperature.

2. Principles of Surface Photovoltage

2.1 [SPV principle]

SPV formally belongs to 'carrier lifetime' methods. These methods are known to be very sensitive, but at the same time very ambiguous, difficult to interpret and very irreproducible. Early round-robin photoconductive decay experiments yielded two-orders-of-magnitude differences in lifetime values obtained in different laboratories on the same samples. These results constituted a clear warning of potential pitfalls⁴⁾. The records of SPV were in this respect much better from the very beginning. The original SPV diffusion length method introduced by Goodman⁵⁾ offered the measurement of true minority carrier bulk parameters free of contributions from surface recombination and from the majority carrier (these parameters are difficult to separate in photoconductive decay). Differences in early round-robin SPV measurements were within 40%⁶⁾. The methods, however, has a potential of absolute accuracy better than 3% and can detect relative changes of 1%.

2.2 [Mechanisms of SPV]

In the SPV method the minority carrier diffusion length is determined from a spectral

dependence of the surface photovoltage ΔV and specially from the dependence of ΔV on the light penetration depth α^{-1} , where α is the absorption coefficient. A depletion- (or inversion- depletion-) type surface barrier (shown in Fig. 1 for an n-type semiconductor) is best suited for measurement⁶⁾.

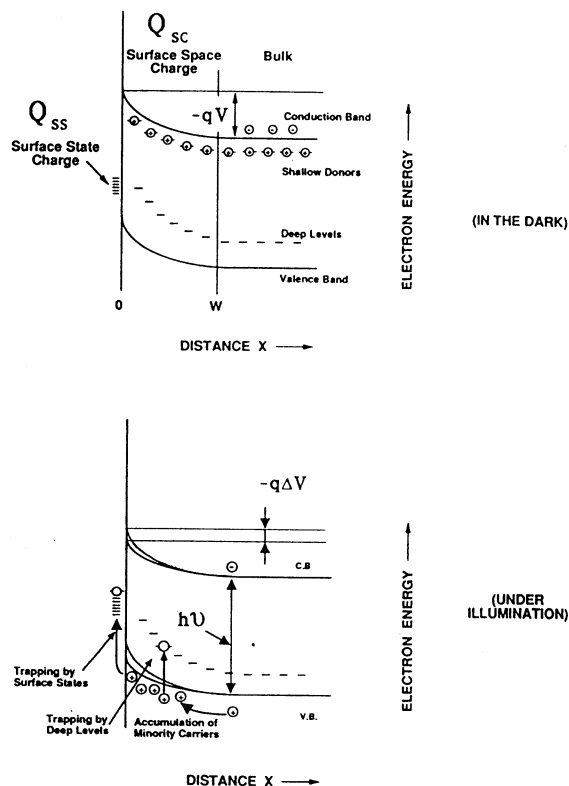


Figure 1 Energy band diagram near an n-type semiconductor surface with a depletion layer in the dark (top) and under illumination (bottom).

This assures preferable collection of the excess minority carriers in the surface space charge, while the majority carriers are repelled from the surface and play an insignificant role. In this method the accumulation of minority carriers should be a predominant mechanism leading to the surface photovoltage. Two additional mechanisms shown at the bottom of Fig. 1, namely trapping of minority carriers by deep levels and trapping by surface states, are essential in non-contact SPV-DLTS⁷⁾. However, they interfere with diffusion length measurement. They introduce hysteresis corresponding to long-time-constant components (in silicon in the range from minutes to 10 ms) of the light-on/light-off SPV relaxations. In the new SPV approach⁸⁾ they are suppressed using light-chopping frequencies in the 500-

600 Hz range, which is high in comparison to the inverse of the surface state time constant. (Note that only about 10 Hz was used in early Goodman approaches and is still erroneously recommended in ASTM procedures^{5,6)}. On the high side the frequency is limited by a decreasing of the photovoltage when $\omega\tau > 1$, where ω is the angular light-chopping frequency and τ is the carrier lifetime. In the new SPV apparatus the hysteresis effects are additionally suppressed using a fast wavelength-changing cycle of the order of 1 s.

The Dember voltage created by the different diffusivities of photoexcited electron and

holes (40 and $10 \text{ cm}^2\text{s}^{-1}$ respectively) is negligible in the linear SPV range, where the excitation level $\Delta n/n_0$ is extremely low (10^{-7} – 10^{-5}).

2.3 [Quantitative SPV equations]

The theoretical calculation of the surface photovoltage is carried out in two independent steps. First, the excess carrier distribution $\Delta p(x)$ is derived from a steady state solution of the continuity equation. For SPV, only the value of Δp just outside the space charge region (at x equal to the space charge width W) is required. This value is given by the standard expression⁹⁾

$$\Delta p = \frac{\Phi_{\text{eff}} \alpha L}{(S + D/L)(1 + \alpha L)} \quad (1)$$

where $\Phi_{\text{eff}} = (1 - R)\Phi$, Φ is the incident photon flux, R is the reflectivity, α is the absorption coefficient, S is the surface recombination velocity on the illuminated front surface and D is the minority carrier diffusivity. It is assumed that the light penetration depth α^{-1} and the diffusion length L are much smaller than the wafer thickness d but much larger than W . The first requirement can often be relaxed to $L < d/2$. The second requirement concerning W is a very stringent one.

In the second calculation step, $\Delta V(\Delta p)$ is derived using the surface-bulk electrical neutrality condition $Q_{\text{sc}} + Q_{\text{ss}} = 0$, where Q_{sc} and Q_{ss} are the space charge density and the surface state charge density respectively¹⁰⁾. It is assumed that under illumination $Q_{\text{ss}} = \text{const}$ and thus $Q_{\text{sc}} = \text{const}$ also. However, under illumination Q_{sc} would tend to increase due to an accumulation of excess holes. Therefore, to maintain Q_{sc} unchanged, the width and also the height of the surface potential barrier must decrease, which leads to the surface photovoltage. ΔV increases with increasing Δp and tends to saturate for $\Delta p \rightarrow \infty$ (when, at the surface, bands become virtually flat). The new SPV approach⁹⁾ uses very low excitation and a linear relationship between ΔV and Δp is fully satisfied (in practice ΔV should be about 1 mV or less). The corresponding analytical expressions have especially simple forms for depleted and inversion surface layers of primary interest here. Using equation(1) and $\Delta V(\Delta p)$ ¹⁰⁾, one gets explicit expressions valid for $\Delta V \ll kt/q$: for the surface depletion layer

$$\Delta V = \Phi_{\text{eff}} \frac{kT}{qn_0} \cdot \frac{\exp(-qV/kT) \alpha L}{(S + D/L)(1 + \alpha L)} \quad (2a)$$

and for the inversion layer

$$\Delta V = \Phi_{\text{eff}} \frac{kT}{qn_i^2} \cdot \frac{n_0 \alpha L}{(S + D/L)(1 + \alpha L)} \quad (2b)$$

where kT is the thermal energy, q is the elementary charge and n_0 and n_i are the free electron concentration in the bulk (no illumination) and the intrinsic free carrier concentration respectively.

Equations (2a) and (2b) have the general form

$$\frac{\Phi_{\text{eff}}}{\Delta V} = A \left(S + \frac{D}{L} \right) \left(1 + \frac{1}{L\alpha^{-1}} \right) \quad (3)$$

where $A = qn_0/kTe \times p(qV/kT)$ for depletion layer and $A = qn_i^2/kTn_0$ for an inversion layer. The last term on the right side of equation (3) is used for determination of L , while the other terms may provide information on the surface parameters S and V .

2.4 [Diffusion length measurements]

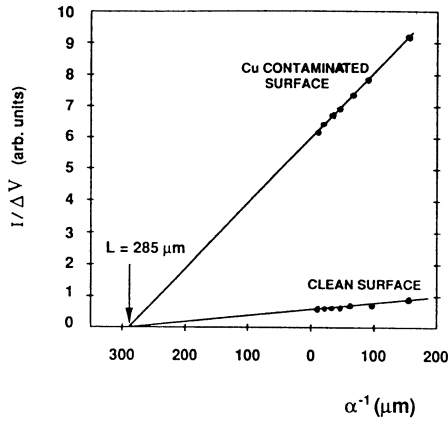


Figure 2 SPV plots, $I/\Delta V$ versus α^{-1} , measured on the same wafer before and after surface contamination with copper. The intercept value determines the diffusion length L , which remains unchanged. The slope of the line increases after contamination owing to the high surface recombination (estimated as $S = 8 \times 10^3 \text{ cm}^{-1}$).

According to equation (3), the diffusion length value can be determined from the linear plot of $\Phi_{\text{eff}}/\Delta V$ versus α^{-1} as $L = \alpha_{\text{int}}^{-1}$, where α_{int}^{-1} corresponds to $\Phi_{\text{eff}}/\Delta V = 0$. In the apparatus based on the new 'constant photon flux SPV method' the effective photon fluxes Φ_{eff} are virtually constant for each wavelength of incident light⁹⁾. Therefore L can be determined from the intercept of the inverse of the surface photovoltage (see Fig. 2). In practice, second-order corrections are used in computation to account for slight difference in Φ_{eff} values. In the data of Fig. 2 these correction are incorporated in the parameter I . The original method proposed by Goodman⁵⁾ was based on the constant magnitude surface photovoltage principle in which photon flux was adjusted

during the measurements to obtain exactly the same ΔV value for each wavelength. Then the diffusion length was determined from the plot of Φ_{eff} versus α^{-1} . This method is more time-consuming and less direct than the new approach. However, the Goodman approach, and his apparatus at the David Sarnoff Research Center, must be acknowledged as a pioneering tool which using the SPV technique¹⁾.

3. Experimental

3.1 [Experimental details]

3.1.1 SPV apparatus

A schematic of the SPV apparatus is shown in Fig. 3. The halogen light source is equipped with a computer-controlled iris for adjusting the photon flux to assure a low-intensity, linear SPV region. Monochromatic light with up to seven pre-selected wavelengths from 1 to $0.8 \mu\text{m}$ is obtained using a narrow bandpass filter wheel driven by a stepping motor. Individual filters are preadjusted to obtain a constant value of the effective photon flux Φ_{eff} at the output of the SPV probe. Typically, Φ_{eff} is constant within $\pm 3\%$ for all wavelengths. Further corrections for Φ_{eff} are incorporated into data-processing software. The filter wheel also incorporates neutral density filters which are used for automatic SPV linearity checking.

SPV values (four-digit accuracy) measured by a two-phase lock-in amplifier are processed in real time by the computer. Wafer mapping is performed digitally using a motor-driven (translation plus rotary) wafer stage. A single-point measurement cycle takes 2-12s depending on the number of wavelengths employed and the lock-in time constant. Wafer mapping containing 177 points with all seven wavelengths and a typical 30ms time constant takes approximately 20 min.

3.1.2 Non-contact SPV

In the non-contact configuration the SPV pick-up probe is placed at a distance d_{pw} , above

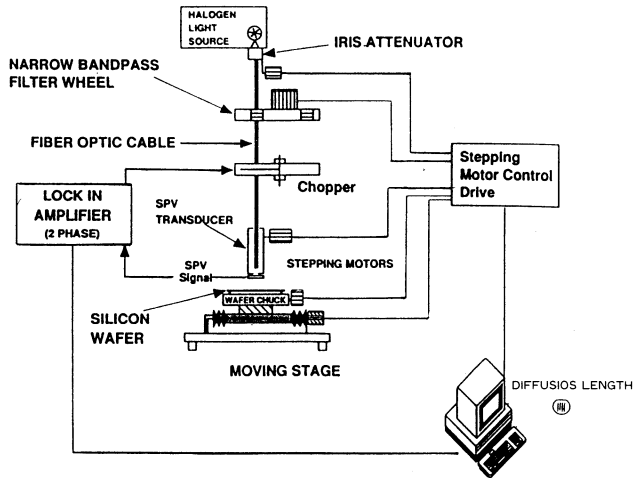


Figure 3 Schematic of the computerized apparatus for SPV mapping.

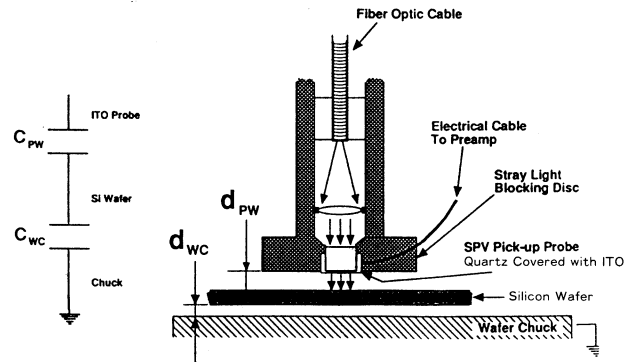


Figure 4 SPV transducer for non-contact measurements and corresponding capacitive coupling.

the silicon wafer, which rests on the supporting pins above the black anodized aluminum wafer chuck (as shown in Fig. 4). The front surface SPV signal is generated on the probe-wafer capacitor C_{pw} . Using a unit-gain FET preamplifier with an input resistance greater than $10^{10}\Omega$, one can perform non-contact SPV measurements even when the probe is 1 cm from the wafer. However, the signal-to-noise ratio increases significantly when d_{pw} is reduced to a fraction of a millimeter. A typical d_{pw} value of 0.2 mm also assures effective blocking of the background light by the probe housing. The contribution from the back-surface photovoltage generated on the wafer-chuck capacitor C_{wc} , is negligible since C_{wc} is typically three orders of magnitude larger than C_{pw} . (Note that d_{pw} is comparable to d_{wc} ; however, the probe diameter of 1-6 mm is much smaller than the silicon wafer diameter of several inches.) The SPV transducer shown in Fig. 4 contains a light-blocking disc which blocks stray light and enables one to carry out measurements with room light present without the need for the dark boxes used in previous SPV approaches.

3.2 Measurement Technique

Lifetime/diffusion length was measured using the SPV method. The constant magnitude SPV method, first proposed by A. Goodman⁵⁾, was initially used to measure diffusion length values. Precision, reproducibility and speed of measurements were recently improved with the introduction of constant photon flux SPV. SPV measurements were performed with commercial Contamination Monitoring System (CMSIII)¹²⁾, manufactured by Semiconductor Diagnostics, Inc., (a single point measurement cycle takes approximately 1 to 4 seconds) with a sensitivity for Fe detection of 10^8 cm^{-3} and were done on product as well as monitor wafers. This allows evaluation of the effects from surface topology, characteristic for a given technology, on cleaning efficiency.

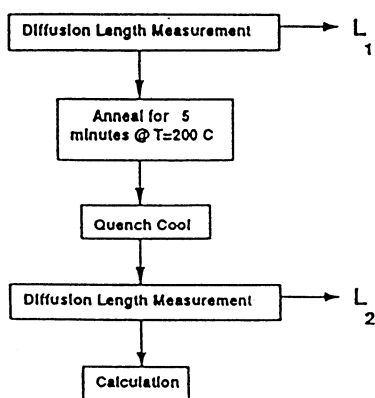
The potential barrier at the surface of the silicon wafer is used as a detector for the photovoltaic effect which is sensed by a non-contact capacitive transducer. During Measurements the SPV signal^{13,14)} is measured as a function of the light penetration depth (wavelength of light) and values of diffusion length and surface recombination are calculated from the spectral dependence of the SPV signal. Measurements are done in a linear range of SPV signal magnitude on light intensity. Since capacitance coupling between the silicon and transducer is used to detect the SPV signal, measurements can be done in a contactless mode on patterned wafers at various stages of processing: oxidation, nitridation, diffusion, plasma treatments, implantation and even after metal definition on wafers, after completion of processing. Measurements are done with very low light intensity in the range of 10^{11} - 10^{13}

photon/cm² per second. Under these conditions, measured values of lifetime are not affected by conditions of measurements and lifetime is inversely proportional to the concentration of heavy metals.

3.3 Sample Preparation

First we measured Fe contamination in p-type silicon. Fe concentration is quantitatively determined from two measurements of diffusion length: prior to and after 200 °C annealing.

CZ silicon wafers (p-type, 6Ω-cm) were prepared by running them through RCA 1, HF dip, and RCA 2 cleaning procedures. The purpose of these steps is twofold. First, it is necessary to remove any surface contamination on as received wafers, and secondly, since we are using aqueous Fe salt contamination solutions, the wafer surface must be hydrophilic. Wafers were then thoroughly rinsed with DI water and dried in centrifuge. Substrates were then placed on a teflon spinner chuck. A solution of iron salts of various concentrations were spilled on the surface, so that it covered the whole surface uniformly, and left on for several minutes. The substrate was then spun dry at 3000 rpm. This procedure is similar to that proposed¹⁵⁾ to introduce a controlled amount of contamination into silicon. We have found that surface concentration is weakly dependent on absorption time for times longer than one minute. Iron was then driven in by rapid thermal processing (PTA) for 90 seconds at 1050 °C in an oxidizing atmosphere. The effectiveness of this procedure was tested by measuring the diffusion length at the front and back surfaces. If they are comparable, then



$$[\text{Fe}] = 1.1 \times 10^{16} \left[\frac{1}{L_2^2} - \frac{1}{L_1^2} \right] \text{ cm}^{-3}$$

Figure 5 Determination of iron concentration using diffusion length measurements.

the substrate is deemed uniformly contaminated. Typically obtained radial uniformity of lifetime is between 8% for heavily contaminated and 25% for lightly contaminated samples. In the case of the highest contamination levels, exceeding $5 \times 10^{13} \text{ cm}^{-2}$ (10^{15} cm^{-3}), drive temperature and time had to be extended to $1150 \text{ }^\circ\text{C}$ for 6 minutes. Iron concentration was measured on all samples via diffusion length analysis. The iron concentration analysis procedure is outlined in Fig. 5 and discussed in detail by Zoth¹⁶). This SPV iron determination method provides an iron detection limit of $1 \times 10^{12} \text{ cm}^{-3}$.

4. Results and Discussion

To establish optimum conditions for the measurement of Fe concentration, diffusion length changes were studied as a function of annealing temperatures, times and temperatures of recovery.

Figure 6 shows diffusion length measured as a function of time in three samples boron concentration of $1 \times 10^{15} \text{ cm}^{-3}$) contaminated by $3 \times 10^{13} \text{ cm}^{-2}$ ($6 \times 10^{14} \text{ cm}^{-3}$), $4 \times 10^{12} \text{ cm}^{-2}$ ($8 \times 10^{13} \text{ cm}^{-3}$) and about $5 \times 10^{11} \text{ cm}^{-2}$ ($1 \times 10^{13} \text{ cm}^{-3}$) of Fe. The samples were annealed at $200 \text{ }^\circ\text{C}$ for 10 minutes and quenched in water to room temperature ($21 \text{ }^\circ\text{C}$) which resulted in a reduction of diffusion length of about three times. The recovery of the diffusion length took place at room temperature. The obser-

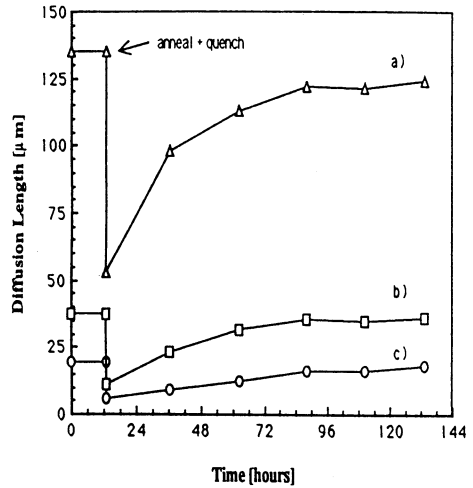


Figure 6 Recovery of minority carrier diffusion length after 10 minutes, $200 \text{ }^\circ\text{C}$ anneal for samples contaminated with three different concentrations of iron: (a) $< 5 \times 10^{11} \text{ cm}^{-2}$; (b) $4 \times 10^{12} \text{ cm}^{-2}$; and (c) $3.3 \times 10^{13} \text{ cm}^{-2}$. Samples were kept at room temperature after annealing. Quenching is marked by the arrow.

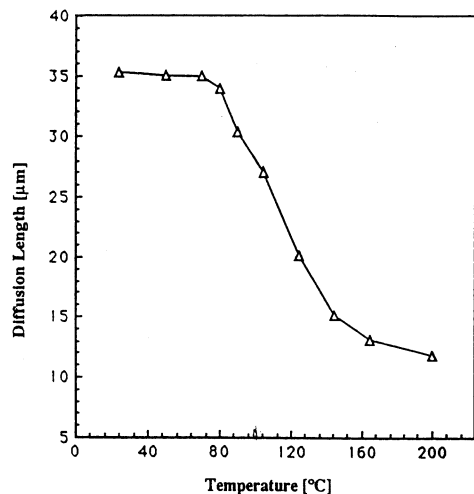


Figure 7 Dependence of diffusion length on annealing temperature.

ved reduction of diffusion length after the 200 °C annealing is caused by decomposition of the Fe-B pairs into interstitial Fe. Since interstitial Fe is in a metastable state at room temperature in p-type silicon, it recombines with boron to form Fe-B pairs which result in a recovery of diffusion length to the initial value. The time required to complete this process at room temperature is about 100 hours. These effects were not observed in either non-contaminated control p-type silicon or in n-type samples.

Figure 7 shows changes in diffusion length as a function of annealing temperature. It appears that Fe-B pairs start to decompose above 100 °C and total decomposition of Fe-B pairs takes place at about 180 °C.

Figure 8 shows the result of a series of diffusion length measurements performed after quenching from 200 °C as a function of recovery temperature. The fastest recovery of Fe-B pairs takes place at 85 °C.

The original value of diffusion length was 35 μm and, after 200 °C annealing, was reduced to 12 μm . The reduction of diffusion length above 100 °C is caused by the beginning of decomposition of Fe-B pairs into interstitial Fe. The observed reduction of diffusion length after a 200 °C annealing is the signature of heavy metal contamination, while the characteristic parameters of the recovery process indicates that the particular element involved in this case is iron. Next Fe contamination, introduced during cleaning, were measured after a high-temperature treatment (a typical oxidation/annealing sequence used during processing or RTA at 1100 °C for 5 minutes) which was used to drive heavy metal left on the surface by the cleaning into the bulk of the wafer. In the case of SPC (Statistical Process Control) of critical steps, e. g., pre-gate cleaning, wafers were measured after the gate oxidation.

The result of various experiments, designed to compare contamination levels for various cleanings, are shown in Fig.9 through 11. The wafers used were p-type, 10 Ω cm and, following cleaning, they were oxidized at 900 °C for 20 minutes. Figure 9 compares various

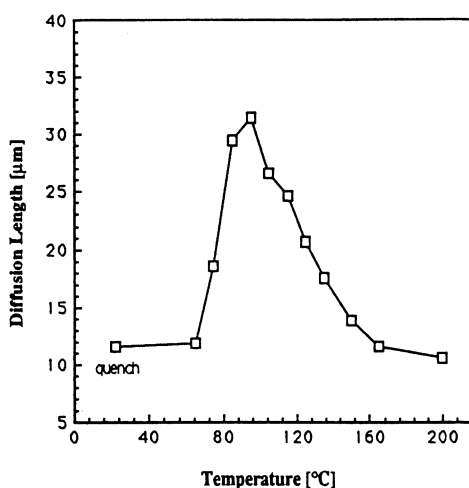


Figure 8 Dependence of diffusion length on sample annealing temperature, after the sample was annealed and quenched.

cleaning methods (MEGA grade chemicals were used). The best results were obtained for the modified SC-1 cleaning (concentration of ammonia was reduced by five times) which also gives the best surface roughness. Figure 10 compares the results for SC-1 and SC-2 cleans for MEGA and SEMI grade chemicals. The MEGA grade chemicals gave about one to two orders of magnitude lower Fe concentration. The results for the SEMI grade chemicals depend very strongly on the shipment since the contamination level in the SEMI grade chemicals exhibits large fluctuations as shown in Fig. 10.

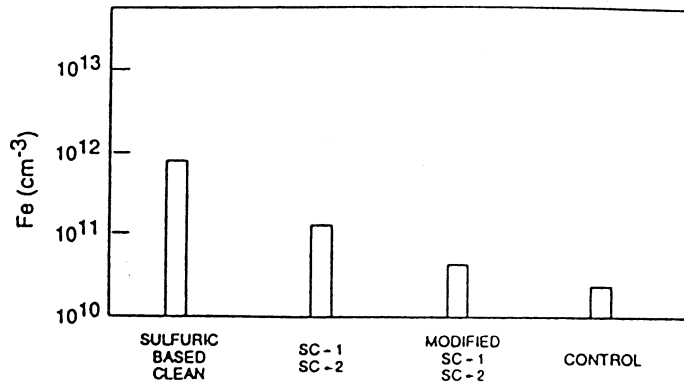


Figure 9 The Fe concentration introduced by various cleans (same grade chemicals).

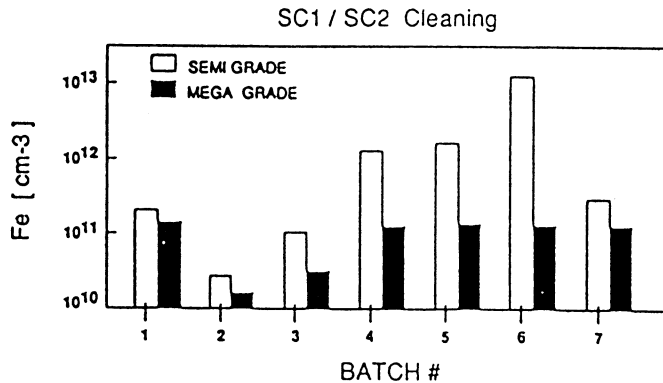


Figure 10 The Fe concentration introduced from MEGA and SEMI grade chemicals as a function of the shipment.

Figure 11 shows the effect of cleaning temperature on the efficiency of the SC-1, SC-2 cleaning process. A decrease in temperature results in a reduction of the Fe concentration (plating of heavy metals from chemicals decreases with temperature), but also an increase in

organic contamination which causes an increase of positive charge in the oxide. There is an optimum temperature for SC-1, SC-2 cleaning steps which is a trade-off between cleaning efficiency for heavy metals and organic contamination.

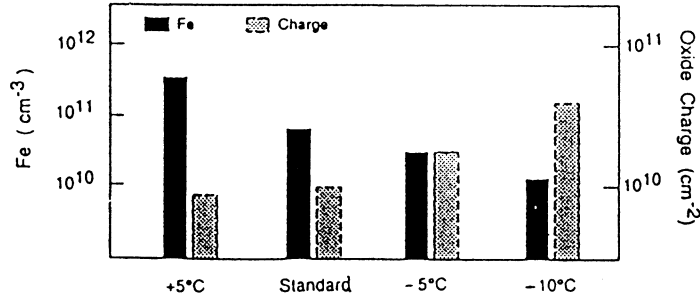


Figure 11 Fe contamination and charge as a function of temperature for SC-1, SC-2 cleaning.

An example of the use of the SPV technique for SPC of pre-oxidation cleaning is shown in Fig. 12. The wafer (p-type, 10Ω cm) were cleaned in a wet chemical sink in which the chemicals were not replaced after each cleaning cycle and oxidized at 900C for 30 minutes. Each point is an average of the Fe measurements after oxidation on two wafers from a 50-wafer lot. The allowable Fe contamination threshold is shown as the dashed horizontal line. Above this level, Fe has a detrimental effect on gate oxide integrity. This SPC chart shows that about eight cleaning runs can be performed before the contamination in the liquid builds up to unacceptable levels and the chemicals have to be replaced.

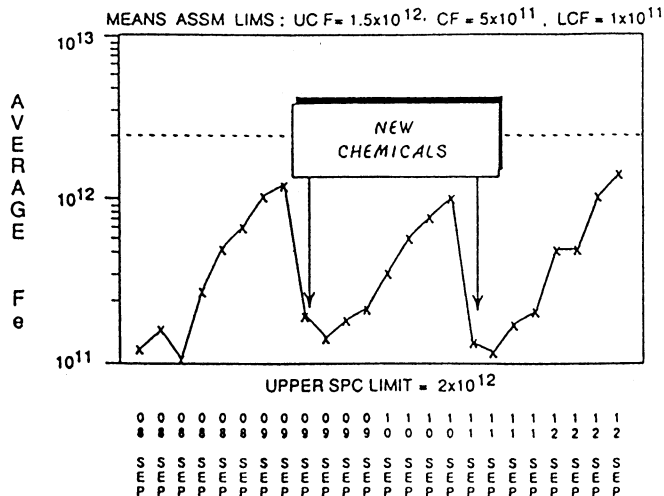


Figure 12 SPC of pre-oxidation wet chemical cleaning (SC-1, SC-2). Chemicals can be reused eight times.

5. Conclusion

This paper presented SPV applications for the monitoring of chemical cleaning and purity of chemicals through mapping of minority carrier diffusion length, Fe concentration in the bulk, and surface contamination (surface charge and surface recombination). The non-contact, wafer-scale character of the new SPV approach, and refined apparatus, make this technique uniquely suited for heavy metal monitoring. To our knowledge no other technique can match this characterization capability. This method was used to monitor Cu contamination in BHF by measurement of its effect on surface recombination and Fe contamination through its effect on bulk recombination after RTA step used to drive Fe deposited at the surface during cleaning into the bulk. Fe surface contamination was measured down to the $1 \times 10^9 \text{ cm}^{-2}$ level while the detection limit of this approach is $2 \times 10^8 \text{ cm}^{-2}$.

The procedure was developed to monitor heavy metal contamination levels in liquid chemicals. Cleanliness of incoming chemicals is not always a limiting factor and often is not related to the cleanliness of chemicals at the point of use (in the cleaning station). Quite often equipment itself can impose serious limitations.

It is apparent that equipment designers could benefit from a better understanding of their equipment performance limitations. The SPV approach is very new compared to more traditional methods such as TXRF and AAS, but has already proven its usefulness in monitoring problems with wet chemistry in IC processing lines. Compared to more traditional methods, the major advantage of SPV measurement is its measurement speed; information is obtained a few minutes after completion of a process step, as well as the capability of carrying out contactless measurements in patterned product wafers.

Acknowledgments

A part of this work was conducted at University of South Florida (USF), which one of the authors (S. N) had spent as overseas researcher of the Ministry of Education, Science and Culture of Japan. We would like to express their appreciation to the various individuals who assisted in sample preparation and data analysis. A special "thank you" goes to Dr. Earl J. Claire, Director of Center for Microelectronics Research Center of USF who has constantly supported this work.

References

- 1) L. Jastrzebski : Semiconductor Silicon 1990, ed. H. R. Huff, K. G. Barraclough and J. Chikaw (Pennington : Electrochemical Society) p. 614.
- 2) A. Ohsawa, K. Honda, R. Takizawa, T. Nakanishi, M. Aoki, N. Toyohura : Semiconductor Silicon 1990, ed. H. R. Huff, Electrochem. Soc., Pennington, NJ, (1990), pp. 601-613.
- 3) G. Zoth : Tech. Proc. SEMICON/Europa, Zurich, March, 1990, p. 23.
- 4) B. Ross : Lifetime Factors in Silicon 1980 (ASTM STP 712) pp. 14-28.
- 5) A. M. Goodman : J. Appl. Phys. **32**, 2550 (1961).
- 6) ASTM STP F391-87, re-approved and extended in 1990 to include the new constant photon flux SPV method.
- 7) J. Lagowski : P. Edelman, and A. Morawski, Semicond. Sci. Technol. **7**, (1992) A211.
- 8) The term 'new SPV approach' refers to the constant photon flux linear SPV method introduced by J. Lagowski (US Patent pending) and implemented in CMS machines manufactured by Semiconductor Diagnostics, Inc.
- 9) T. S. Moss : J. Electron. Control, **1**, 126 (1995).
- 10) E. O. Johnson : J. Appl. Phys., **28**, 1349 (1957).
- 11) This range corresponds to the most reliable silicon absorption coefficient data ; see M. Saritas and H. D. McKell : J. Appl. Phys., **63**, 4561 (1988).
- 12) Model CMSIII-A manufactured by Semiconductor Diagnostics Inc. of Tampa, Florida.
- 13) J. Lagowski, U. S. Patent 5, 025, 145, issued June 1991.
- 14) J. Lagowski, P. Edelman, M. Dexter, W. Henley : Proc. of Defect Recognition and Imaging in Semiconductors before and after Processing (DRIP4) Conf., Mottram St. Andrews, England, March 1991.
- 15) M. Fujimo, K. Hiramoto, M. Sano, K. Murakami, H. Horiyo, Y. Oka and S. Sumita : Semiconductor Silicon 1990, ed. H. R. Huff, Electrochem. Soc., Pennington, NJ, (1990), p. 720.
- 16) G. Zoth and W. Bergholz : J. Appl. Phys., **67**, (11) 6764 (1990).